

PAPER • OPEN ACCESS

Developments in multiple-valve water-hammer control

To cite this article: A Bergant *et al* 2021 *IOP Conf. Ser.: Earth Environ. Sci.* **774** 012008

View the [article online](#) for updates and enhancements.

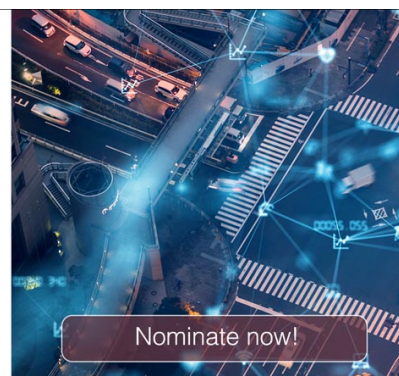


The Electrochemical Society
Advancing solid state & electrochemical science & technology

The ECS is seeking candidates to serve as the
Founding Editor-in-Chief (EIC) of ECS Sensors Plus,
a journal in the process of being launched in 2021

The goal of ECS Sensors Plus, as a one-stop shop journal for sensors, is to advance the fundamental science and understanding of sensors and detection technologies for efficient monitoring and control of industrial processes and the environment, and improving quality of life and human health.

Nomination submission begins: May 18, 2021



Developments in multiple-valve water-hammer control

A Bergant^{1,2}, S Hässig³, U Karadžić⁴, K Urbanowicz⁵, A Tijsseling⁶

¹ Litostrój Power d.o.o., 1000 Ljubljana, Slovenia (Full-Time)

² University of Ljubljana, 1000 Ljubljana, Slovenia (Part-Time)

³ ETH Zurich, 8092 Zurich, Switzerland

⁴ University of Montenegro, 81000 Podgorica, Montenegro

⁵ West Pomeranian University of Technology, Szczecin 70-310, Poland

⁶ Eindhoven University of Technology, 5600 MB Eindhoven, The Netherlands

Corresponding author's e-mail address: anton.bergant@litostrójpower.eu

Abstract. This paper investigates multiple-valve closures in a simple reservoir-valve-pipeline-valve system. Multiple closing (or opening) of valves may induce large positive or low negative pressure waves due to wave interference (superposition of the waves). The effect of multiple-valve closure can be either beneficial or detrimental, with the outcome being entirely dependent on the position of the valves and the sequence and delay of the closures. Valves are incorporated as boundary conditions in the method of characteristics model. The staggered (diamond) grid with consideration of unsteady skin friction is applied. Experimental investigations of multiple-valve induced water-hammer have been performed in the University of Montenegro laboratory pipeline apparatus. The apparatus consists of an upstream end high-pressurized tank, horizontal steel pipeline (length 55.37 m, inner diameter 18 mm), four valve units positioned along the pipeline including the end points, and a downstream end tank. The transient event is initiated first by rapid closure of the downstream-end valve followed by the delayed closure of the upstream-end valve. Calculated and measured results are compared and discussed in the light of the effects of pressure wave interference.

1. Introduction

Water hammer may induce large pressure pulsations and pipeline vibrations. Most of the academic water-hammer research has been done for the classical case of single-valve closure in a simple reservoir-pipeline-valve system [1], [2]. However, there is a large number of pipelines with multiple-valves (hydropower, water supply, process industry), at least with two of them (one at the upstream end and one at the downstream end). Simultaneous (or with a small delay) closing (or opening) of valves may produce high or low transient pressures due to the superposition of waves travelling in opposite directions (interference). The effect of multiple-valve closure can be either beneficial or detrimental [3], [4], with the outcome being entirely dependent on the position of the valves and the sequence of the closures [5], [6], [7]. This paper presents recent results from the authors' theoretical and experimental work on multiple-valve water-hammer control (pure liquid flow). The selected piping system is a simple reservoir-valve-pipeline-valve system (two-valve system). The system with two closing far-end valves generates two water-hammer waves that interfere at some point along the pipeline. Because the two waves are water-hammer waves, the two-valve system equipped with pressure control system can be referred to as a *water-hammer interferometer* [8].



Valves are incorporated as boundary conditions in the method of characteristic numerical scheme (MOC). The staggered (diamond) grid with consideration of unsteady skin friction is applied. Experimental investigations of multiple-valve induced water-hammer have been performed in the University of Montenegro laboratory pipeline apparatus. The apparatus consists of an upstream end high-pressurized tank, horizontal steel pipeline (length 55.37 m, inner diameter 18 mm, pipe wall thickness 2 mm), four valve units positioned along the pipeline including the end points, and a downstream end tank. The transient event is initiated first by rapid closure of the downstream-end valve followed by the delayed closure of the upstream-end valve. Different valve closure sequences are first investigated in an ideal frictionless system with instantaneous valve closures to identify typical pressure histories. The paper concludes with analysis of two distinct experimental runs. Measured and calculated results are compared and discussed in the light of the effects of wave interactions.

2. A note on theoretical modelling

Water-hammer theory describes the propagation of pressure waves in pipelines. The standard procedure to solve the water-hammer equations of motion and continuity is the method of characteristics (MOC) [1], [9]. The standard MOC solution is based on simplified water-hammer equations (the convective transport terms are neglected). The dependent variables pressure p and flow velocity V (cross-sectionally averaged velocity) are traditionally replaced by piezometric head H and discharge Q . This procedure yields two water-hammer compatibility equations that are valid along characteristic lines in the distance-time plane. Their standard finite-difference form within the staggered grid of the MOC is:

- compatibility equation along the C^+ characteristic line ($\Delta x/\Delta t = a$):

$$H_{i,t} - H_{i-1,t-\Delta t} + \frac{a}{gA} ((Q_u)_{i,t} - Q_{i-1,t-\Delta t}) + \frac{f\Delta x}{2gDA^2} (Q_u)_{i,t} |Q_{i-1,t-\Delta t}| = 0 \quad (1)$$

- compatibility equation along the C^- characteristic line ($\Delta x/\Delta t = -a$):

$$H_{i,t} - H_{i+1,t-\Delta t} - \frac{a}{gA} (Q_{i,t} - (Q_u)_{i+1,t-\Delta t}) - \frac{f\Delta x}{2gDA^2} Q_{i,t} |(Q_u)_{i+1,t-\Delta t}| = 0 \quad (2)$$

Section 7 explains the symbols. At a boundary (reservoir, valve) a device-specific equation replaces one of the compatibility equations [1], [9].

2.1 Unsteady friction

The steady (or quasi-steady) friction (skin friction) term is traditionally incorporated in the MOC algorithm. This assumption is satisfactory for slow transients where the wall shear stress has a quasi-steady behaviour. Previous investigations using the quasi-steady friction approximation for rapid transients have shown significant discrepancies in attenuation, shape and timing of pressure traces when computational results were compared with measurements [10]. The MOC based algorithm used in this paper incorporates a convolution-based (with quasi-2-D weighting function) unsteady friction model [11]. The unsteady frictional head loss per unit length h_f is formulated by the following term:

$$h_f = \frac{f_0}{2gDA^2} Q|Q| + \frac{16\nu}{gD^2A} \left(\frac{\partial Q}{\partial t} * W_0(t) \right) \quad (3)$$

in which "*" represents convolution. The subscript "0" denotes parameter values based on the steady-state condition preceding the transient event. The Darcy-Weisbach relation (first term) defines the steady-state component and the unsteady component (second term) is defined by the convolution of a weighting function with past accelerations ($\partial Q/\partial t$). The weighting function W_0 is based on an assumed steady-state viscosity distribution preceding the transient event, which is kept constant during the event (the "frozen viscosity" assumption) [12]. An accurate and efficient *Urbanowicz* approximate scheme [13] that does not require *convolution* with the complete history of velocities required at each time step is used in this paper.

3. Laboratory pipeline apparatus

A small-scale pipeline apparatus has been designed and constructed at the University of Montenegro for investigating water-hammer events including multiple-valve closures. The apparatus is comprised of a horizontal steel pipeline that connects the upstream-end high-pressure tank to the outflow tank (total length $L = 55.37$ m; internal diameter $D = 18$ mm; pipe wall thickness $e = 2.0$ mm; maximum allowable pressure in the pipeline $p_{max, all} = 25$ MPa) – see Figure 1.

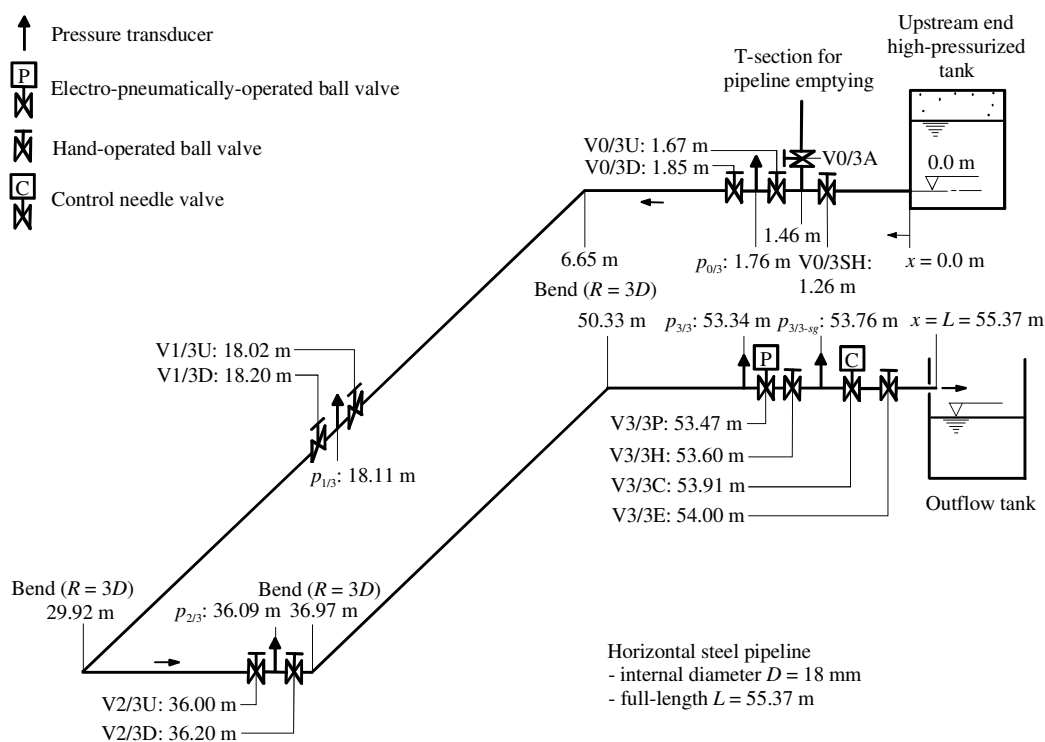


Figure 1. Layout of small-scale pipeline apparatus.

Four valve units are positioned along the pipeline including the end points (valves $V^*/3^*$ at positions 0/3, 1/3, 2/3 and 3/3). The air pressure in the upstream-end tank can be adjusted up to 800 kPa (gauge). The pressure in the tank is kept constant during each experimental run by using a high-precision fast-acting air pressure regulator (precision class: 0.2%) in the compressed-air supply line. Four dynamic high-frequency pressure transducers are positioned within the valve units along the pipeline including the end points (see Figure 1). Pressures $p_{0/3}$, $p_{1/3}$, $p_{2/3}$ and $p_{3/3}$ are measured by Dytran 2300V4 high-frequency piezoelectric absolute pressure transducers (pressure range: from 0 to

6.9 MPa; resonant frequency: 500 kHz; acceleration compensated; discharge time constant: 10 seconds (fixed); uncertainty: $\pm 1\%$). The datum level for all pressures measured in the pipeline and at the tank is at the top of the horizontal steel pipe (elevation 0.0 m in Figure 1). The downstream-end valves V3/3P and V3/3H are equipped with fast-response displacement sensors Positek P500.90BL (measurement range: from 0 to 90°; frequency response: 10 kHz; uncertainty: $\pm 0.5^\circ$). The sensors measure the change of the valve angle during valve closing and opening. The initial flow velocity V_0 is measured with different methods. For initial flow velocities larger than 0.3 m/s an electromagnetic flow meter (Krohne OPTIFLUX 4000F IFC 300C) is used. Smaller steady-state velocities are estimated from the Joukowski pressure head rise or drop resulting from the rapid valve action. In addition, the initial velocity may be measured by a volumetric method (checking and calibration of electronically-based metering). The estimated uncertainty in velocity measurement is $\pm 1\%$. The water temperature is continuously monitored by the thermometer installed in the outflow tank (uncertainty: $\pm 0.5^\circ\text{C}$). The water-hammer wave speed was determined as $a = 1340 \pm 10$ m/s.

3.1. Test procedure for multiple-valve closure event

The test procedure is as follows. The steady-state flow conditions (in advance of a dynamic test) are controlled by a set pressure in the upstream-end tank and by a set opening of the downstream-end control needle valve (valve V3/3C in Figure 1). The water level in the upstream-end pressurized tank can be adjusted. From initial steady flow conditions, a transient event is initiated by downstream-end (V3/3H) or/and upstream-end (V0/3U) valve closures by hand (single- or multiple-valve action).

4. Numerical and experimental results

This section presents results from distinct numerical and experimental runs in the laboratory small-scale pipeline apparatus (Figure 1). Transients were induced first by a fast closure of the downstream-end valve V3/3H and second by a delayed fast closure (including simultaneous one) of the upstream-end valve V0/3U. First we investigate numerical results for the case of ideal flow conditions (frictionless system, instantaneous closure of the two valves) [8]. Second, computed results are compared with the results of measurements for the case of delayed fast closure of the upstream-end valve V0/3U.

4.1 Ideal system

Numerical results are presented for an ideal test apparatus assuming instantaneous closure of the two valves in a frictionless system. Pressure head traces are depicted in dimensionless form at the downstream end ($x/L = 1$), at the midpoint ($x/L = 1/2$) and at the upstream end of the pipe system ($x/L = 0$). It should be noted that the dimensionless head traces are the same for any similar pipeline system. Figure 2 presents results for the case of simultaneous two-valve closure (valves V3/3H and V0/3U) and for several typical cases of delayed closure of the upstream-end valve V0/3U (time delay: $0 < t_d \leq 4L/a$).

Simultaneous two-valve closure (Figure 2a) produces pressure head variations at the two far-end valves with a period of $2L/a$ (two times higher frequency ($a/2L$) than that for the classical single-closure case ($a/4L$; [9])). The head at the midpoint remains constant at all times (the waves are cancelled out (wave destruction)). When the closure of the valve V0/3U delays for $0.5L/a$, the heads at the two far-end valves vary with a period of $2L/a$ – Figure 2b. The pressure head at the midpoint exhibits variation with a period of L/a (four times higher frequency than that for the classical single-closure case) and it never drops below the initial static head (halving the peak-to-peak pressure head amplitude). The delayed closure by L/a of V0/3U shows no oscillations – Figure 2c. Instead, the head is trapped (accumulated) at the positive Joukowski pressure head ($H = H_0 + (a/g)V_0$) at all times. The delayed closure of the upstream-end valve V0/3U at a time $1.5L/a$ after closure of V3/3H shows a similar response as the delayed closure of V0/3U by a time of $0.5L/a$. The flow situation induced by the delayed upstream-end valve closure at time $2L/a$ after the downstream-end valve closure (Figure

2d) is somehow similar to the situation of simultaneous valve closure (Figure 2a). Wave interference produces pressure head variations at the two far-end valves with a period of $2L/a$, whereas the head at the midpoint remains constant at all times. Naturally, the head response within $0 \leq t \leq 2L/a$ is the classical single-valve closure response.

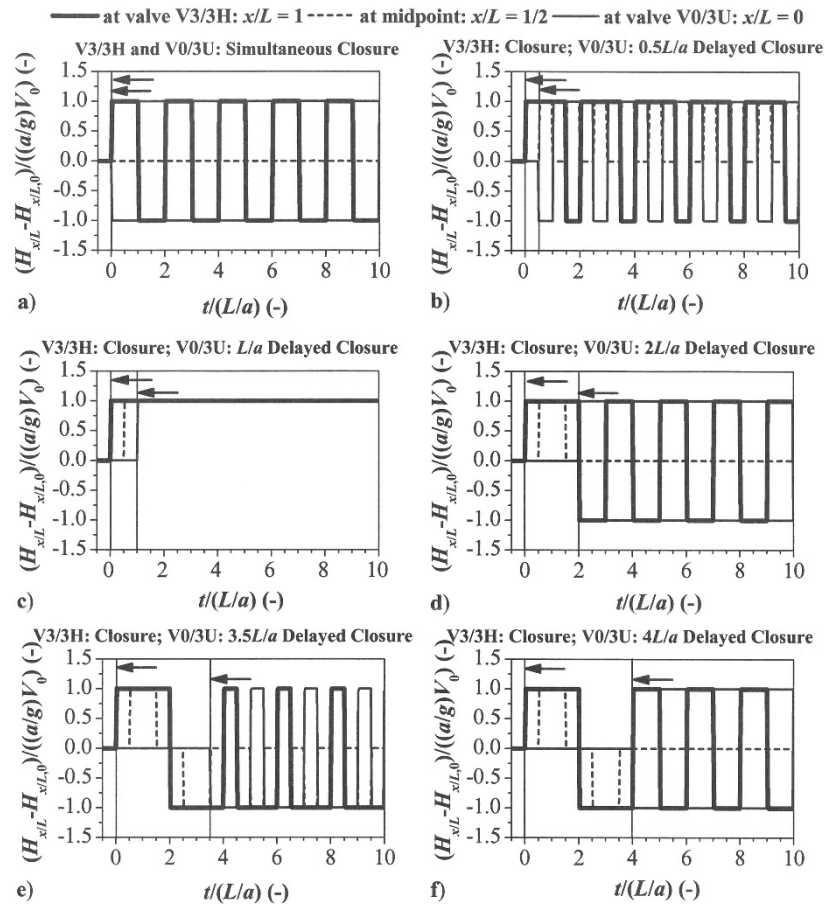


Figure 2. Typical dimensionless head histories in the frictionless test apparatus: Instantaneous closure of the end valves, first V3/3H and then V0/3U (time delay: $0 \leq t_d \leq 4L/a$).

The situation for the case of delayed closure of the valve V0/3U with time delays ranging from $2L/a$ to $4L/a$ is reversed (change of sign). This holds both for delayed closures of V0/3U by times $2.5L/a$ and $3.5L/a$ (Figure 2e), and by time $3L/a$ (in this case the pressure head in the pipeline is $H = H_0 - (a/g)V_0$). Again, the flow situation induced by delayed closure of V0/3U at time $4L/a$ after closure of V3/3H (Figure 2f) is in a way similar to the situation of simultaneous valve closure (Figure 2a) and $2L/a$ delayed closure (Figure 2d). Wave interference after the second valve closure (simultaneous or delayed for $n2L/a$; $n = 1, 2, 3 \dots$) produces head variations at the far-end valves with a period of $2L/a$, whereas the head at the midpoint remains constant at all times. In essence, the complete wave response is comprised of two parts: (1) single-valve response before the second valve closure and (2) two-valve response after the delayed second valve closure (V0/3U in our case). Simultaneous valve closure can be considered as a limit case. The delayed closure of the second valve has a profound effect on the pressure head responses in the pipeline system (increased frequency of pulsation, cancellation of waves (neutral, positive or negative accumulation)).

4.2 Measured and computed results

A number of experiments have been performed in the laboratory apparatus (Figure 1). The valve closures were induced ‘simultaneously’ as much as possible by using the valve V3/3H at the downstream end of the pipeline and the valve V0/3U at the upstream end. Results from two distinct experimental runs are presented and compared with calculated results in this section: (1) water hammer with delayed closure of V0/3U at time $t_d = 46$ ms ($1.15L/a$) and (2) water hammer with delayed closure of V0/3U at time $t_d = 150$ ms ($3.75L/a$). The number of computational reaches in all runs was $N = 96$ and the wave speed was $a = 1340$ m/s. The sampling frequency for each continuously measured quantity was $f_s = 3,000$ Hz.

Figure 3 presents measured and computed pressure head traces ($H_{3/3}$, $H_{2/3}$, $H_{1/3}$ and $H_{0/3}$) for the rapid closure of the two valves with delayed closure of V0/3U at time $t_d = 46$ ms ($1.15L/a$). The initial flow velocity was $V_0 = 0.31$ m/s and the static pressure in the upstream-end pressurized reservoir was $p_{res} = 400$ kPa. The valve closure times $t_c = 30$ ms of V3/3H and $t_c = 25$ ms of V0/3U were much less than the wave return time $2L/a = 80$ ms. The fast closure of the downstream-end valve (V3/3H) produces the classical Joukowski pressure head rise $\Delta H_{max} = 42$ m. The second delayed fast closure of the upstream-end valve (V0/3U) produces a pressure head rise at this valve of practically the same magnitude. The delayed closure of $1.15L/a$ of V0/3U shows only small oscillations. It is similar to the ideal case with delayed closure of L/a of V0/3U, where the accumulated head is the positive Joukowski pressure head ($H = H_0 + (a/g)V_0$) at all times (Figure 2c). The imperfections due to different valve closure times (hand closure, not instantaneous) and pipe-wall friction are not ideal; however, they do allow head accumulation as in the ideal case. There is reasonable agreement between measured and computed results.

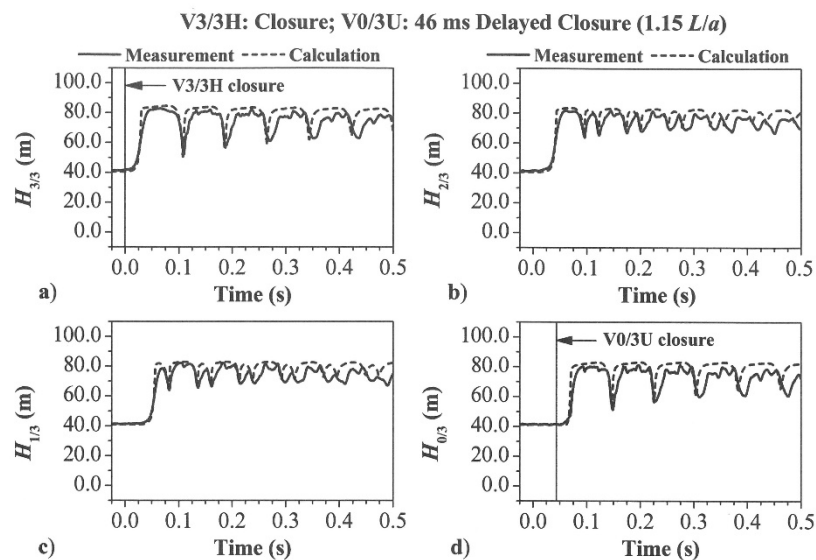


Figure 3. Comparison of measured and calculated heads at two end valves ($H_{3/3}$ and $H_{0/3}$) and along the pipeline ($H_{2/3}$ and $H_{1/3}$): $V_0 = 0.31$ m/s; $p_{res} = 400$ kPa.

The second case study presents measured and computed pressure head traces for the fast closure of the two valves with delayed closure of V0/3U at time $t_d = 150$ ms ($3.75L/a$) – see Figure 4. The initial flow velocity was $V_0 = 0.32$ m/s and the static pressure in the upstream-end pressurized reservoir was $p_{res} = 400$ kPa. The valve closure times $t_c = 30$ ms of V3/3H and $t_c = 26$ ms of V0/3U were much less than the wave return time $2L/a = 80$ ms. The fast closure of the downstream-end valve (V3/3H) produces the classical Joukowski pressure head rise $\Delta H_{max} = 44$ m. For this case, the second delayed fast closure of the upstream-end valve (V0/3U) produces a pressure head drop at this valve of similar

magnitude. When the closure of the valve V0/3U delays for $3.75L/a$, the heads at the two far-end valves as well as at one- and two-third points along the pipe vary with a period of $2L/a$. Pressure heads along the pipe never exceed the initial static head (halving the peak to peak pressure head amplitude). The head histories are similar to the ideal case heads with the delayed closure of V0/3U at time $3.5L/a$. The only difference is that the ideal midpoint head oscillates with a frequency of a/L due to the superposition of waves (Figure 2e). Again, the imperfections due to different valve closure times (hand closure, not instantaneous) and pipe-wall friction are not ideal; however, they exhibit the same peak-to-peak amplitudes as in the ideal case. The computed and measured results agree reasonably well.

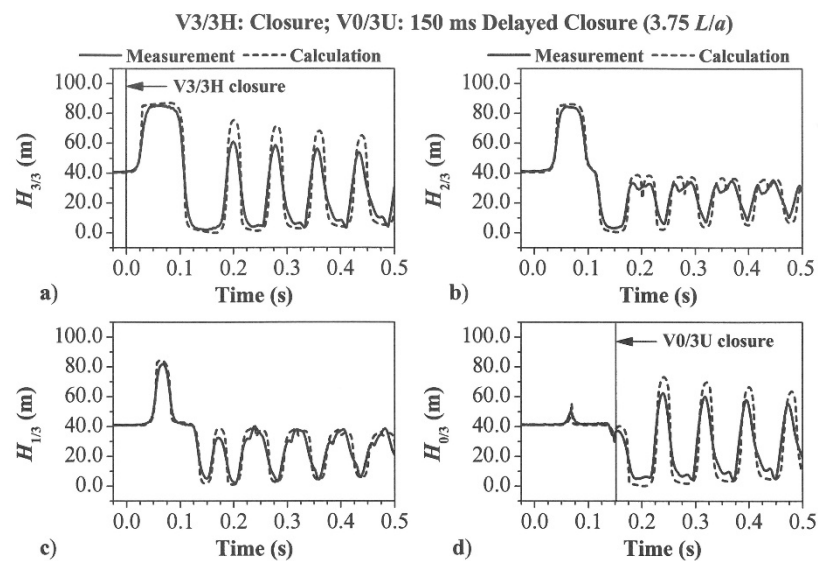


Figure 4. Comparison of measured and calculated heads at two end valves ($H_{3/3}$ and $H_{0/3}$) and along the pipeline ($H_{2/3}$ and $H_{1/3}$): $V_0 = 0.32$ m/s; $p_{res} = 400$ kPa.

5. Conclusions

This paper investigates the effects of multiple-valve closure in a simple reservoir-valve-pipeline-valve system (two-valve system). The two valves can be closed either simultaneously or with time delay. The system with two rapid closing far-end valves generates two water-hammer waves that superimpose (interfere) at some point along the pipeline. The waves are correlated or coherent with each other. This may produce larger or lower pressure heads with different frequencies depending on the valve control scenario. Moreover, the delayed closure of the upstream-end valve with a delay of L/a results in no oscillations in the pipeline. Instead, the head is trapped (accumulated) at a positive or negative Joukowski pressure head at all times. The time delay of closure of the second valve has a profound effect on the pressure head traces in the pipeline system. Calculated and measured results agree reasonably well. Finally, the imperfections due to different actual valve closure times (non-instantaneous hand closure) and pipe-wall friction slightly deteriorate measured pressure histories from the ideal ones. The two-valve closure device (water-hammer interferometer) is a powerful means to control transient pressures in pipeline systems.

6. References

- [1] Wylie E B and Streeter V L 1993 *Fluid Transients in Systems* (Englewood Cliffs: Prentice-Hall)
- [2] Thorley A R D 2004 *Fluid Transients in Pipeline Systems. A Guide to the Control and Suppression of Fluid Transients in Liquids in Closed Conduits* (London and Bury St. Edmunds: Professional Engineering Publishing Limited)
- [3] Ikeo S, Kobori T 1975 Water hammer caused by valve stroking in a pipe with two valves *Bulletin of JSME* **18** pp 1151-1157
- [4] Bergant A, van 't Westende J M C, Koppel T, Gale J, Hou Q, Pandula Z and Tijsseling A S 2010 Water hammer and column separation due to accidental simultaneous closure of control valves in a large scale two-phase flow experimental test rig *Proceedings of the ASME Pressure Vessels and Piping Division Conference (Bellevue, Washington, USA)* Paper PVP2010-26131
- [5] Liu Y, Huang Z, Jiang C 2015 Characteristics of water hammer induced valve-valve system *International Conference on Fluid Power and Mechatronics (Harbin)* (New York: IEEE) 5 p
- [6] Bergant A and Karadžić U 2015 Developments in valve-induced water-hammer experimentation in a small-scale pipeline apparatus *Proceedings of the 12th International Conference on Pressure Surges (Dublin)* (Cranfield: BHR Group) pp 639-652
- [7] Karadžić U, Janković M, Strunjaš F, Bergant A 2018 Water hammer and column separation induced by simultaneous and delayed closure of two valves *Strojniški vestnik - Journal of Mechanical Engineering* **64** pp 525-535
- [8] Bergant A 2016 Principles of water hammer interferometer *Journal of Energy Technology* **9** pp 11-20
- [9] Chaudhry M H 2014 *Applied Hydraulic Transients* (New York: Springer)
- [10] Bergant A, Simpson A R and Vítkovský J 2001 Developments in unsteady pipe flow friction modelling *Journal of Hydraulic Research* **39** pp 249-257
- [11] Zielke W 1968 Frequency-dependent friction in transient pipe flow *Journal of Basic Engineering* **90** pp 109-115
- [12] Vardy A E, Brown J M B, He S, Ariyaratne C, Gorji S 2015 Applicability of frozen-viscosity models of unsteady wall shear stress *Journal of Hydraulic Engineering* **141** Paper 04014064
- [13] Urbanowicz K 2018 Fast and accurate modelling of frictional transient flow *Zeitschrift für Angewandte Mathematik und Mechanik* **98** pp 802-823

7. List of symbols

A	pipe area	Q	discharge
a	wave speed	Q_u	upstream-end discharge
C^+, C^-	label of characteristic equations	R	pipe radius
D	pipe diameter	t	time
e	pipe-wall thickness	t_c	valve closure time
f	friction factor	t_d	time delay
f_s	sampling frequency	V	average flow velocity
g	gravitational acceleration	W	weighting function
H	piezometric head (head)	x	distance along pipe
h_f	head loss per unit length	ΔH	head rise
L	length	Δt	time step
N	number of reaches	Δx	space step
p	pressure (gauge)	ν	kinematic viscosity

Subscripts:

<i>i</i>	node number	<i>res</i>	reservoir
<i>max</i>	maximum	0	initial conditions

Abbreviations:

MOC method of characteristics

ACKNOWLEDGEMENTS

The authors gratefully acknowledge the support of the Slovenian Research Agency (ARRS) conducted through the project L2-1825 and the programme P2-0126.